a reduced threshold voltage upon reimmersion. Electrowetting is by definition an attractive interaction between mercury and SWNT and, thus, the force required to pull a SWNT off a mercury surface should be larger in an activated state than that of a nonactivated state (*36*).

Electrowetting in carbon nanotubes may offer opportunities for studies of nanofluidic transport. It can also be exploited for the formation of continuous nanowires crystallized in one dimension from low–melting point metals (e.g., Ga and In), enabling the measurement of the intrinsic electrical and magnetic properties of encapsulated nanowires. Such structures, attached to AFM tips, could serve as robust nanoelectrode probes with increased current load capacity and enhanced imaging capabilities.

References and Notes

1. Y. Gogotsi, J. A. Libera, A. Güvenc-Yazicioglu, C. M. Megaridis, *Appl. Phys. Lett.* **79**, 1021 (2001).
2. D. Ugarte, A. Chatelain, W. A. de Heer, *Science* **274**, 1897 (1996).
3. P. M. Ajayan, S. Iijima, *Nature* **361**, 333 (1993).
4. C. Guerret-Plecourt, Y. Le Bouar, A. Loiseau, H. Pascard, *Nature* **372**, 761 (1994).
5. C. H. Kiang, J. S. Choi, T. T. Tran, A. D. Bacher, *J. Phys. Chem. B* **103**, 7449 (1999).
6. S. C. Tsang, Y. K. Chen, P. J. F. Harris, M. L. H. Green, *Nature* **372**, 159 (1994).
7. T. W. Ebbesen, *J. Phys. Chem. Solids* **57**, 951 (1996).
8. P. M. Ajayan, T. W. Ebbesen, *Rep. Prog. Phys.* **60**, 1025 (1997).
9. M. Monthioux, *Carbon* **40**, 1809 (2002).
10. E. Dujardin, T. W. Ebbesen, H. Hiura, K. Tanigaki, *Science* **265**, 1850 (1994).
11. E. Dujardin, T. W. Ebbesen, A. Krishnan, M. M. J. Treacy, *Adv. Mater.* **10**, 1472 (1998).
12. S. Frank, P. Poncharal, Z. L. Wang, W. A. de Heer, *Science* **280**, 1744 (1998).
13. N. R. Wilson, D. H. Cobden, J. V. Macpherson, *J. Phys. Chem. B* **106**, 13102 (2002).
14. P. Poncharal, C. Berger, Y. Yi, Z. L. Wang, W. A. de Heer, *J. Phys. Chem. B* **106**, 12104 (2002).
15. M. W. J. Prins, W. J. J. Welters, J. W. Weekamp, *Science* **291**, 277 (2001).
16. L. A. Wade, I. R. Shapiro, Z. Ma, S. R. Quake, C. P. Collier, *Nano Lett.* **4**, 725 (2004).
17. J. H. Hafner, C.-L. Cheung, T. H. Oosterkamp, C. M. Lieber, *J. Phys. Chem. B* **105**, 743 (2001).
18. Materials and methods are available as supporting material on *Science* Online.
19. To measure conductance, the probe is reimmersed into mercury and the current is measured at low bias (100 mV).
20. G. Lippmann, *Ann. Chim. Phys.* **5**, 494 (1875).
21. The exact mechanism of charge buildup at the SWNT-mercury interface is not known, but it is thought to be caused by a tunneling barrier to electrons in a direction perpendicular to the SWNT center axis (*37*).
22. N. K. Adam, *The Physics and Chemistry of Surfaces* (Dover, New York, 1968).
23. We never found any solid or liquid material inside as-grown nanotubes despite extensive TEM imaging of hundreds of nanotubes grown by our chemical vapor deposition technique.
24. A. Awasthi, Y. J. Bhatt, S. P. Garg, *Meas. Sci. Technol.* **7**, 753 (1996).
25. M. Fialkowski, P. Grzeszczak, R. Nowakowski, R. Holyst, *J. Phys. Chem. B* **108**, 5026 (2004).
26. R. E. Hummel, *Int. Mater. Rev.* **39**, 97 (1994).
27. After activation, the measured high currents suggest large power dissipation, most likely occurring at both contacts. Thermomigration is not expected to contribute appreciably to mass transport from the Hg bath to the AFM tip, if both contacts become hot.
28. B. C. Regan, S. Aloni, R. O. Ritchie, U. Dhamen, A. Zettl, *Nature* **428**, 924 (2004).
29. The Hg bath consists of 37,013 mercury atoms. Periodic boundary conditions are applied in the *x* and *y* directions, and the size of simulation domain is 10.8 by 10.4 nm. The liquid is positioned on top of a layer of fixed Hg atoms, and the SWNT is initially placed outside the bath. After equilibration at 300 K, the SWNT is lowered into the liquid at a constant speed of 10 m/s while the liquid is maintained at 300 K. Carbon-carbon interactions in the walls are omitted to decrease the time of computation.
30. S. Supple, N. Quirke, *Phys. Rev. Lett.* **90**, 214501 (2003).
31. We perform the calculation at a potential larger than the calculated threshold (2.5 V) for electrowetting of the (20,20) SWNT to speed up the wetting and filling. Calculated thresholds increase with nanotube diameter and are generally larger than those seen experimentally.
32. The quadratic scaling can be predicted through the Lucas-Washburn equation by introducing a velocity-dependent dynamic contact angle or, correspondingly, a "wetting-line friction" as proposed by Martic *et al*. (*38*).
33. To estimate the amount of the dissolved Au, we assume a pyramidal AFM tip with conformal Au coating, which terminates into a spherical apex. We also assume that 30% of the Au atoms in the remaining Au coating with the lighter contrast have formed an amalgam.
34. The simulation predicts that mercury will rapidly drain from the (20,20) SWNT core at a speed of 15 m/s when the applied potential is decreased to zero.
35. The work function of Au (5.1 eV) is greater than that of Hg (4.6 eV) and the amalgam value should be in between (*39*).
36. A nonwetting condition is always repulsive. The weak pull-off force measured at voltages below threshold must be a result of extraneous effects such as adsorbed water. It is important to focus on the difference in pull-off force before and after activation.
37. B. Shan, K. Cho, *Phys. Rev. B* **70**, 233405 (2004).
38. G. Martic *et al.*, *Langmuir* **18**, 7971 (2002).
39. H. B. Michaelson, *J. Appl. Phys.* **48**, 4729 (1977).

40. We thank C. Garland for TEM assistance. Supported in part by NSF (grants CTS-0404353 and CTS-0508096) and in part by the Arrowhead Research Corporation.

Supporting Online Material

www.sciencemag.org/cgi/content/full/310/5753/1480/DC1
Materials and Methods
Figs. S1 to S6
Tables S1 and S2
References

20 September 2005; accepted 1 November 2005
10.1126/science.1120385

A Well-Preserved *Archaeopteryx* Specimen with Theropod Features

Gerald Mayr,[1]* Burkhard Pohl,[2] D. Stefan Peters[1]

A nearly complete skeleton of *Archaeopteryx* with excellent bone preservation shows that the osteology of the urvogel is similar to that of nonavian theropod dinosaurs. The new specimen confirms the presence of a hyperextendible second toe as in dromaeosaurs and troodontids. *Archaeopteryx* had a plesiomorphic tetraradiate palatine bone and no fully reversed first toe. These observations provide further evidence for the theropod ancestry of birds. In addition, the presence of a hyperextendible second toe blurs the distinction of archaeopterygids from basal deinonychosaurs (troodontids and dromaeosaurs) and challenges the monophyly of Aves.

The Archaeopterygidae from the Late Jurassic of Germany are recognized as the earliest undisputed fossil avians (*1*, *2*). Archaeopterygids have been known from nine skeletal specimens (*3*, *4*), and most of these are fragmentary or poorly preserved. As a result, crucial features of their osteology have remained uncertain or entirely unknown (*3*, *5*).

Here we describe a 10th skeletal specimen of an archaeopterygid (*3*, *4*). The specimen was discovered in an unknown locality of the Solnhofen area and was housed in a private collection before it was recently acquired by the Wyoming Dinosaur Center, Thermopolis, USA (collection number WDC-CSG-100; a cast will be deposited in Forschungsinstitut Senckenberg).

The "Thermopolis specimen" is a slightly dissociated skeleton on a single slab of pure limestone. Wing and tail feather impressions are well preserved (Fig. 1). In size and osteology, the new specimen corresponds best with the Munich specimen, which is the holotype of *Archaeopteryx bavarica* (*6*) (table S1). However, because there is an ongoing controversy about the taxonomic composition of the Archaeopterygidae, which currently include two genera, *Archaeopteryx* and *Wellnhoferia* (*3*, *7*), we do not assign the new specimen to a particular species in the present study.

The skull is the best-preserved one of all archaeopterygids and the only one that is exposed in dorsal view. There are two accessory antorbital openings, which were recognized in the Eichstätt specimen but whose presence was recently questioned (*3*, *8*). They are part of the maxillary bone (*9*, *10*) and not

[1]Forschungsinstitut Senckenberg, Division of Ornithology, Senckenberganlage 25, D-60325 Frankfurt am Main, Germany. [2]Wyoming Dinosaur Center, 110 Carter Ranch Road, Post Office Box 912, Thermopolis, WY 82443, USA.

*To whom correspondence should be addressed. E-mail: Gerald.Mayr@senckenberg.de

of the mesethmoid (*2*), and thus are homologous to the maxillary and promaxillary fenestrae of theropod dinosaurs (*11*, *12*) (Fig. 2).

The dorsal surface of the midsection of the right palatine bone is visible through the antorbital fenestra (Fig. 2). Apart from minor differences in proportions, this bone closely resembles the isolated palatine of the holotype of the Munich specimen (*13*). However, in contrast to the latter, it also exhibits a short jugal process (Fig. 2) and is thus tetraradiate as in nonavian theropods and not triradiate as in ornithurine birds. Because we do not think that there was such a great morphological discrepancy between the otherwise similar specimens, and because there appears to be a breakage line in the holotype of the Munich specimen, we assume that part of the lateral margin of the palatine of the Munich specimen is broken.

The ectopterygoid is preserved in its original position (*8*), and the hook-shaped jugal process contacts the jugal. The temporal region is difficult to interpret and apparently not completely preserved, because neither a squamosal nor a quadratojugale (*13*) can be discerned.

Nearly the entire right coracoid is visible in cranial view, a bone whose shape in *Archaeopteryx* has been uncertain and of which remarkably different reconstructions exist (*2*, *14*, *15*). The body is of subrectangular shape and bent craniocaudally, with a concave lateral margin and a well-developed lateral process (Fig. 3). In its shape it resembles the

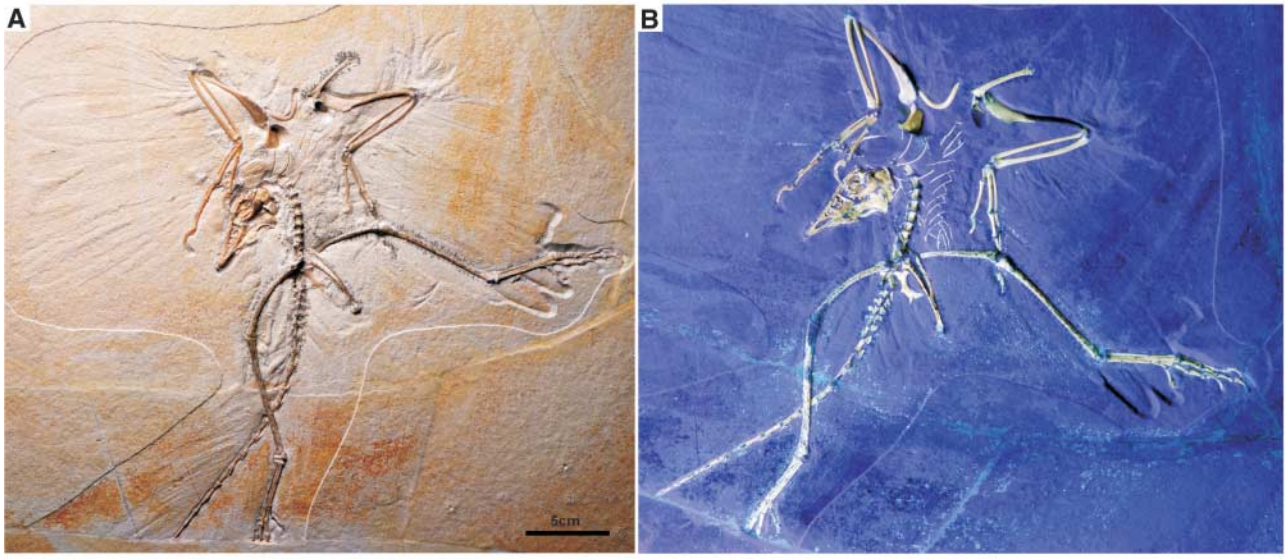

Fig. 1. The 10th skeletal specimen of the Archaeopterygidae (collection number WDC-CSG-100) in ventral view. (**A**) Skeleton with wing and tail feather impressions. (**B**) Ultraviolet-induced fluorescence photograph to show the preserved bone substance.

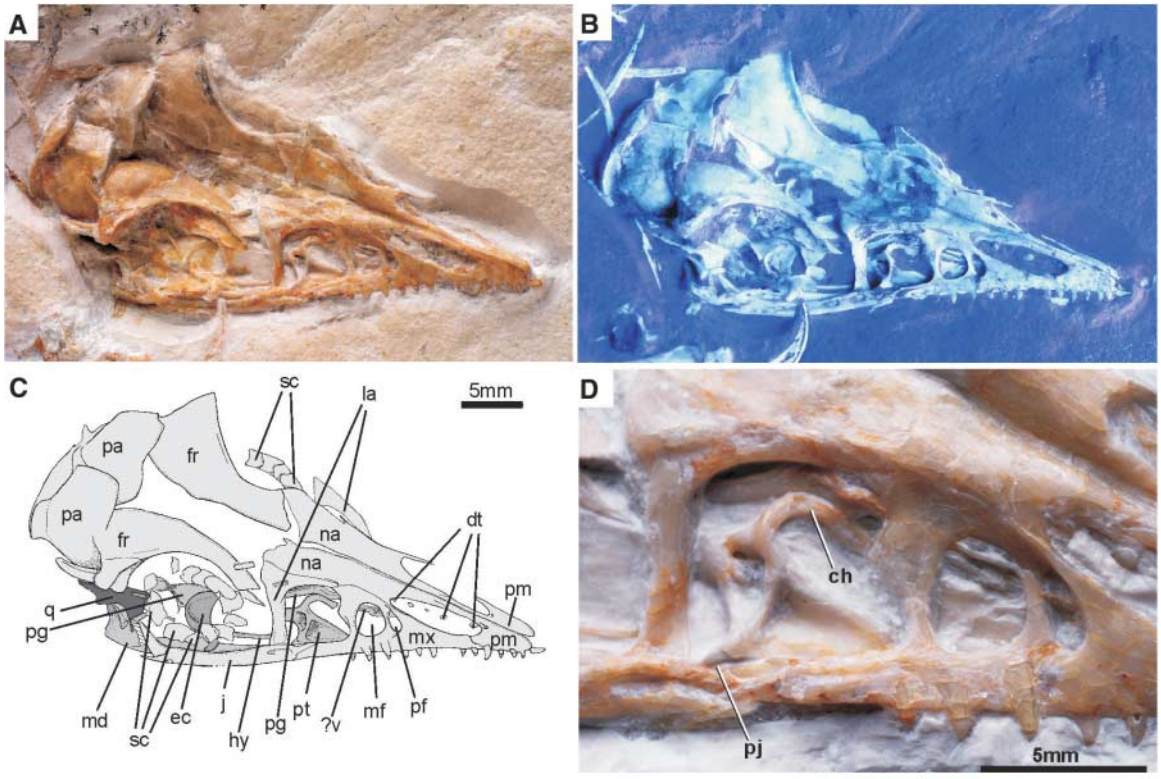

Fig. 2. Skull of the new *Archaeopteryx* specimen. (**A**) Overall view as preserved. (**B**) Ultraviolet-induced fluorescence photograph. (**C**) Interpretative drawing. ch, choanal process of palatine; dt, dentary teeth; ec, ectopterygoid; fr, frontal; hy, hyoid; j, jugal; la, lacrimal; md, mandible; mf, maxillary fenestra; mx, maxilla; na, nasal; pa, parietal; pf, promaxillary fenestra; pg, pterygoid; pj, jugal process of palatine; pm, praemaxilla; pt, palatine; q, quadrate; sc, plates of sclerotic ring; ?v, ?vomer. (**D**) Detail of antorbital fenestra with palatine bone.

coracoid of dromaeosaurs (*1*), although the biceps tubercle is more strongly developed. Coracoid and scapula are not fused, and in concordance with other specimens of the Archaeopterygidae (*14*), there are no ossified sternal plates.

The structure of the proximal tarsal bones of *Archaeopteryx* has played a role in discussions about the theropod ancestry of birds, with the controversy being about whether *Archaeopteryx* had an ascending process of the astragalus as in nonavian theropod dinosaurs (*1*, *16*) or whether there was a narrow "pretibial bone" as in neognathous birds (*2*, *17*–*19*). The new specimen shows the undistorted cranial surface of the tarsus. It is clearly visible that the astragalus forms a broad ascending process identical to that of theropod dinosaurs (*1*) (Fig. 3).

Contrary to virtually all existing reconstructions of *Archaeopteryx*, the new specimen shows that the first toe was not fully reversed as in extant birds. On both feet, the first metatarsal attaches to the medial surface of the second metatarsal as in theropod dinosaurs, not to its plantar surface as in extant birds with a retroverted first toe (*20*). The shaft of the first metatarsal does not exhibit the torsion that is characteristic of birds with a fully retroverted first toe (*20*). The proximal phalanx of the first toe further exposes its mediodorsal surface (Fig. 3). Because the metatarsals are visible in dorsal view, the dorsal aspect of this phalanx would not be visible if the first toe were fully reversed. All pedal phalanges are firmly articulated, and postmortal dislocation is unlikely to affect both feet in the same way. We thus conclude that the first toe of *Archaeopteryx* was spread medially and not permanently reversed as in extant birds. It has hitherto been unrecognized that the first toe exhibits the same position in the only preserved foot of the holotype of the recently established archaeopterygid taxon *Wellnhoferia* (*21*, *22*). In this specimen, the metatarsals are seen from their plantar side and the proximal phalanx of the first toe from its medioplantar side. The first toe of the left foot of the Berlin specimen also appears to have been spread medially rather than having been fully reversed. The feet of the London and Eichstätt specimens are preserved in lateral or medial view, and the impression of a reversed first toe in these specimens may thus be an artefact of preservation, because the medially spread toe is brought on a level with the sedimentation layer.

The absence of a fully reversed first toe indicates that *Archaeopteryx* did not have a perching foot and was at best facultatively arboreal (*3*).

In addition, the new specimen shows that *Archaeopteryx* had a hyperextendible second toe, as in Deinonychosauria (dromaeosaurs and troodontids) and the late Cretaceous bird *Rahonavis* (*12*, *23*). Although the proximal phalanx of the second toe of *Archaeopteryx* is not as abbreviated as in the latter three taxa (*3*), the ability to hyperextend this toe is clearly indicated by the proximodorsally expanded articular trochlea of its first phalanx (Fig. 3). The second toe bears a larger claw than the other digits, which is, however, not as greatly enlarged as in most (*24*) Deinonychosauria. This observation confirms the controversial presence of a dorsally expanded articular trochlea of the proximal phalanx of the second toe in the Eichstätt specimen (*3*, *11*, *24*). Whether its apparent absence in the London *Archaeopteryx* (*25*) is real or an artifact of preservation needs to be further examined; the dorsal part of the trochlea of the second toe of the other specimens is either not visible or is too poorly preserved for detailed examination.

Most workers consider Deinonychosauria to be the sister taxon of Aves (*26*–*28*), and the presence of a hyperextendible second toe in *Archaeopteryx* supports a close relationship between deinonychosaurs and avians. On the basis of current phylogenies (*26*–*28*), this feature must be regarded as an apomorphy of a clade (Deinonychosauria + Avialae) that is lost in birds that are closer to the extant species than are archaeopterygids and *Rahonavis*.

In order to evaluate how the data obtained from the new specimen affect the phylogenetic position of *Archaeopteryx*, we corrected char-

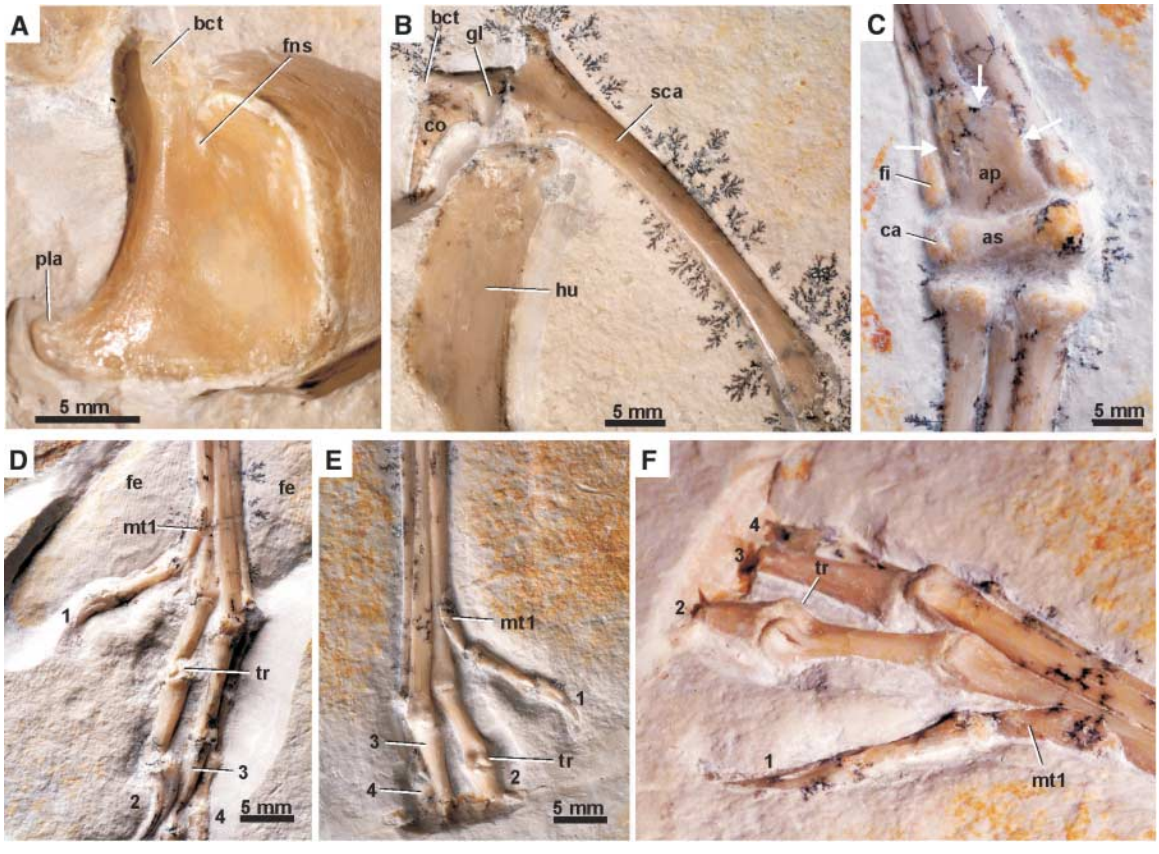

Fig. 3. Selected postcranial bones of the new *Archaeopteryx* specimen. (**A**) Right coracoid in cranial view. (**B**) Left coracoid in lateral view, proximal end of left humerus in caudal view, and left scapula in lateral view. (**C**) Right tarsus in cranial view. (**D**) Left foot in dorsal view. (**E** and **F**) Right foot in dorsal (E) and dorsomedial (F) view. as, astragalus; ap, ascending process of astragalus; bct, biceps tubercle; ca, calcaneus; co, coracoid; dt, dentary teeth; fe, feather impressions; fi, fibula; fns, foramen nervi supracoracoidei; gl, glenoid process of coracoid; hu, humerus; mt1, first metatarsal; pla, lateral process of coracoid; sca, scapula; tr, proximodorsally expanded articular trochlea of first phalanx of second toe. White arrows in (C) indicate the margins of the ascending process of the astragalus; pedal digits are numbered in (D) to (F).

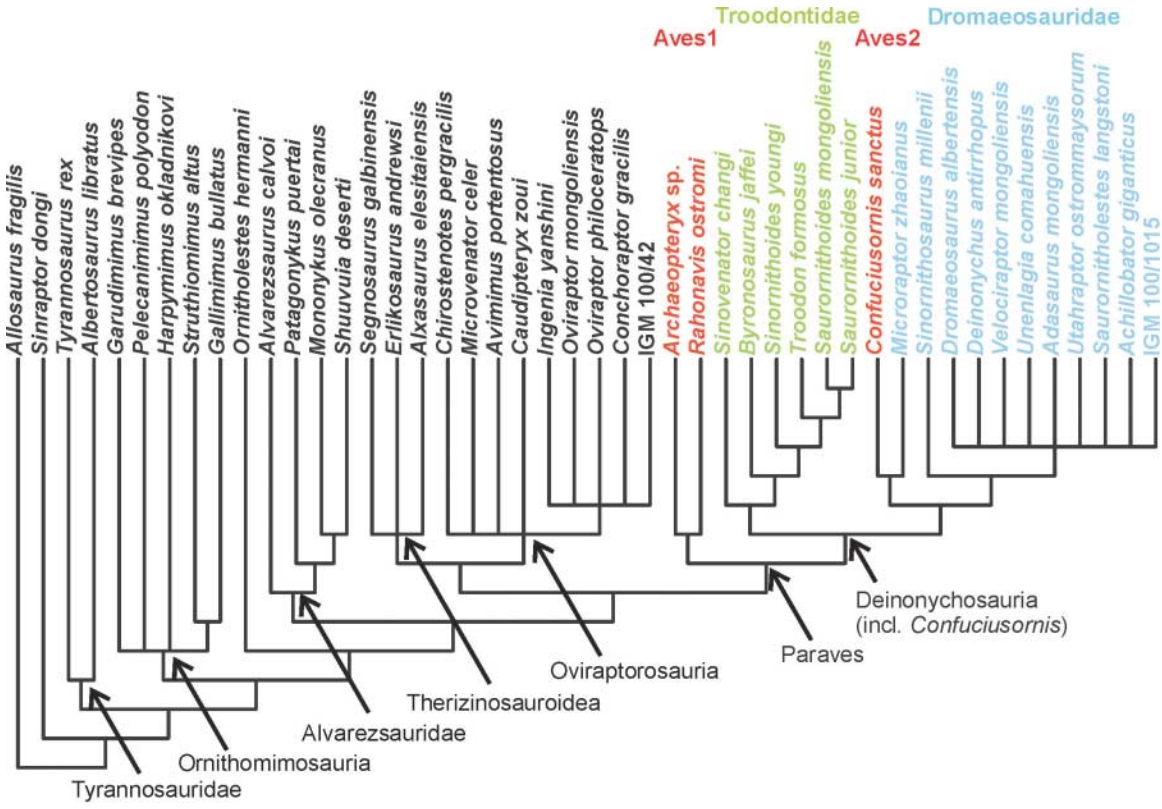

Fig. 4. Strict consensus tree of 288 most parsimonious trees (length, 599; consistency index, 0.42; retention index, 0.70) resulting from a phylogenetic analysis of the character matrix of (*26*) with NONA 2.0 (*29*). Eight characters were modified for *Archaeopteryx* as follows, according to our results and those in (*13*, *14*) [character (ch.) numbers refer to (*26*); character states and descriptions in brackets refer to the scoring used in this analysis): ch. 28:0 [quadratojugal L-shaped (*13*)], ch. 48:0 [palatine tetraradiate], ch. 106:– [not applicable, as there are no ossified sternal plates in the adult (*14*)], ch. 111:? [coracoid and scapula are unfused in most specimens, but fusion may have occurred in late ontogeny (*3*)], ch. 163:1 [ascending process of astragalus separated by transverse groove from condylar portion], ch. 166:0 [metatarsals not co-ossified], ch. 170:2 [newly added character state: penultimate phalanx of digit II modified for hyperextension but ungual not hypertrophied], ch. 171:0 [metatarsal I articulates to medial surface of metatarsal II]. One character was further modified for *Rahonavis*: ch. 111:0 [scapula and coracoid separate (*23*)]. Settings of the analysis and all other scorings are as in (*26*); *Allosaurus fragilis* and *Sinraptor dongi* were used as outgroup taxa. Character scoring for all taxa is given in the supporting online material.

acter scoring for this taxon in large character matrices that include birds and nonavian theropods (*26*) (Fig. 4). Reanalysis of the data did not support monophyly of the three included avian taxa but showed *Archaeopteryx* and *Rahonavis* to be outside a clade including *Confuciusornis* and Deinonychosauria. The analysis further resulted in a sister group relationship between *Confuciusornis* and *Microraptor*, which is generally considered to be a basal dromaeosaur (*26*). Although this particular result may be due to the limited sampling of avian taxa, the presence of a deinonychosaurian key feature (a hyperextendible second toe) and the absence of two avian key features [a triradiate palatine (*3*) and a fully reversed first toe] in *Archaeopteryx* challenges the monophyly of Aves as currently recognized. There are no significant derived characters that are exclusively shared by *Archaeopteryx* and more typical avians such as *Confuciusornis* but are absent in basal deinonychosaurs such as *Microraptor*. The latter and *Confuciusornis* also share a number of derived features that are absent in *Archaeopteryx*, including ossified uncinate processes (optimized as a synapomorphy of the clade including *Confuciusornis* and deinonychosaurs in our analysis), an ulna that is much wider than the radius [not included in the matrix of (*26*)], and a plantarly situated first metatarsal (recovered as a synapomorphy of *Confuciusornis* + *Microraptor* in our analysis) (*26*). Thus Aves, if defined as the clade including *Archaeopteryx* and modern birds, may actually include taxa hitherto referred to as "deinonychosaurs" (*24*), some of which had fully developed avian-type wing feathers (*27*).

References and Notes

1. J. H. Ostrom, *Biol. J. Linn. Soc.* **8**, 91 (1976).
2. L. D. Martin, in *Origins of the Higher Groups of Tetrapods: Controversy and Consensus*, H.-P. Schultze, L. Trueb, Eds. (Comstock, Ithaca, NY, 1991), pp. 485–540.
3. A. Elżanowski, in *Mesozoic Birds: Above the Heads of Dinosaurs*, L. M. Chiappe, L. Witmer, Eds. (Univ. of California Press, Berkeley, CA, 2002), pp. 129–159.
4. M. Röper, *Archaeopteryx* **22**, 1 (2004).
5. L. M. Chiappe, *Nature* **378**, 349 (1995).
6. P. Wellnhofer, *Archaeopteryx* **11**, 1 (1993).
7. P. Senter, J. H. Robins, *J. Vertebr. Paleontol.* **23**, 961 (2003).
8. A. Elżanowski, *Neth. J. Zool.* **51**, 207 (2001).
9. P. Wellnhofer, *Palaeontographica* **147**, 169 (1974).
10. L. M. Witmer, *Zool. J. Linn. Soc.* **100**, 327 (1990).
11. J. A. Gauthier, in *The Origin of Birds and the Evolution of Flight*, K. Padian, Ed. (California Academy of Sciences, San Francisco, CA, 1986), pp. 1–55.
12. D. B. Weishampel, P. Dodson, H. Osmólska, *The Dinosauria* (Univ. of California Press, Berkeley, CA, 2004).
13. A. Elżanowski, P. Wellnhofer, *J. Vertebr. Paleontol.* **16**, 81 (1996).
14. P. Wellnhofer, H. Tischlinger, *Archaeopteryx* **22**, 3 (2004).
15. G. de Beer, Archaeopteryx lithographica. *A Study Based upon the British Museum Specimen* [British Museum (Natural History), London, 1954].
16. J. H. Ostrom, in *Origins of the Higher Groups of Tetrapods: Controversy and Consensus*, H.-P. Schultze, L. Trueb, Eds. (Comstock, Ithaca, NY, 1991), pp. 467–484.
17. L. D. Martin, J. D. Stewart, K. N. Whetstone, *Auk* **97**, 86 (1980).
18. S. Tarsitano, in *Origins of the Higher Groups of Tetrapods: Controversy and Consensus*, H.-P. Schultze, L. Trueb, Eds. (Comstock, Ithaca, NY, 1991), pp. 541–576.
19. L. Martin, in *The Beginnings of Birds*, M. K. Hecht, J. H. Ostrom, G. Viohl, P. Wellnhofer, Eds. (Freunde des Jura-Museums Eichstätt, Eichstätt, Germany, 1985), pp. 177–183.
20. K. M. Middleton, *J. Morphol.* **250**, 51 (2001).
21. A. Elżanowski, *Acta Palaeontol. Pol.* **46**, 519 (2001).
22. P. Wellnhofer, *Los Angeles City Mus. Nat. Hist. Sci. Ser.* **36**, 3 (1992).
23. C. A. Forster, S. D. Sampson, L. M. Chiappe, D. W. Krause, *Science* **279**, 1915 (1998).
24. G. S. Paul, *Dinosaurs of the Air: The Evolution and Loss of Flight in Dinosaurs and Birds* (Johns Hopkins Univ. Press, Baltimore, MD, 2002).
25. A. Elżanowski, Ł. Paśko, *Acta Ornithol.* **34**, 123 (1999).
26. S. H. Hwang, M. A. Norell, H. Gao, *Am. Mus. Novitat.* **3381**, 1 (2002).
27. X. Xu *et al.*, *Nature* **421**, 335 (2003).
28. P. C. Sereno, *Science* **284**, 2137 (1999).
29. P. A. Goloboff, *NONA version 2.0* (computer program), S. M. de Tucumán, Argentina (1993).

30. We thank A. Manegold for discussions, S. Hwang for her data matrix, S. Tränkner for taking the photographs, F. F. Steininger for acting as an intermediary enabling us to study the fossil, D. Unwin for access to the Berlin specimen, and A. Elżanowski and two anonymous referees for comments on the manuscript.

Supporting Online Material

www.sciencemag.org/cgi/content/full/310/5753/1483/DC1
SOM Text
Table S1

19 September 2005; accepted 31 October 2005
10.1126/science.1120331